Laboratory Study of Add-On Treatments for Interior Noise Control in Light Aircraft

John S. Mixson,* Louis A. Roussos,† and C. Kearney Barton‡
NASA Langley Research Center, Hampton, Virginia
and
Rimas Vaicaitis§ and Mario Slazak¶
Columbia University, New York, New York

This paper describes experimental and theoretical studies of transmission loss of 1.15 × 1.46-m flat panels of skin-stiffener construction having damping, fiberglass, or double-wall add-on acoustic treatments. Results were obtained in a laboratory facility consisting of adjacent hardwall rooms, using space averages in the reverberant source and receiving rooms. Results indicate that the effectiveness of each treatment varies with frequency, with most treatments performing better at high frequency. The measured increase of transmission loss is substantially different for different combinations of treatment and the heavier of two treatments did not always provide the greater increase of transmission loss. Theoretical results are in fair agreement with measurements, and the theory is used along with data extrapolation to design side walls for a noise control example.

Introduction

SUBSTANTIAL levels of interior noise in light aircraft arise from engine and propeller noise that is transmitted through the fuselage side-wall structure. In order to reduce the cabin noise, improved side-wall attenuation (increased transmission loss) is expected to be required in addition to reductions of source noise levels. Recent theoretical studies have examined the feasibility of interior noise control using "add-on" treatments such as damping tape, fiberglass layers, septa, honeycomb stiffness, and double walls.[1-3] The results have been encouraging and suggest that such treatments can be designed in appropriate combinations to provide the required noise reduction. Add-on treatments have been studied experimentally using aircraft[4]; however, the complications of testing with aircraft limit the number of treatments that can be investigated and sometimes obscure the effect of the treatment. The laboratory study described herein was undertaken to define the noise transmission variables for a number of treatments and to verify the theories for application to light aircraft side walls.

Acoustic Tests

Experiments were carried out in the facility illustrated in Figs. 1 and 2. The facility was designed[5] around two existing adjacent rooms, one of which, the receiving room, is acoustically and structurally isolated from the rest of the building.

As shown in the figures, the "window" between the two rooms can accommodate test specimens that are similar in size to light aircraft fuselage side walls.

The instrumentation for the facility consists of a rotating boom microphone in each room (Fig. 2), two reference sound power source fans in the source room, a digital one-third octave band analyzer, a desk top computer, and digitally operated relays. The computer is programmed to start and stop the sound sources, switch microphones for the analyzer, and operate the analyzer, with the result that the entire measurement procedure is automatically controlled. Broadband noise is generated in the source room and sound pressure levels in source and receiving rooms are averaged over space and time. The difference in sound levels, the noise reduction (NR), is related to transmission loss (TL) by

$$TL = NR + 10 \log (S/A) \quad (1)$$

where S is the area of the test specimen and A is the absorption in the receiving room. The receiving room absorption was determined from tests of a 4.66-kg/m^2 rubber sheet.[6] Measured NR and calculated field incidence mass law TL (determined by the normal incidence TL minus 5 dB method[7]) were used in Eq. (1) to calculate values of absorption that were then used in the remaining tests.

Test Panel and Acoustic Treatments

The aluminum test panel and acoustic treatments are illustrated in Figs. 3 and 4. The panel shown in Fig. 2 has nominally the same dimensions of skin and stiffeners as the panel tested (Fig. 3). The dimensions are intended to be representative of light aircraft construction. Acoustic treatments (Fig. 4) consisted of a fiberglass-septum combination, a foam-foil damping layer, and a plywood trim panel. Nine configurations were tested using various combinations of these treatments (Table 1).

Dimensions of the stiffener cross sections are shown in Fig. 4. The panel was clamped in the test window as shown in Fig. 2 using 2.54-cm-wide steel straps and bolts on 10.2-cm centers. The dimensions of the panel are 115 × 146 cm measured

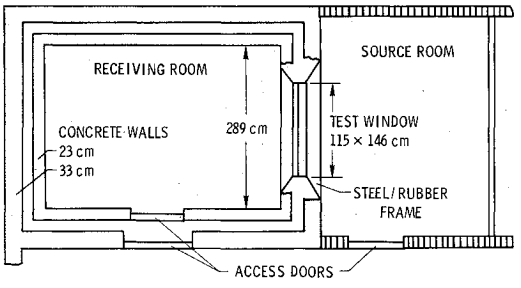

Fig. 1 Plan view of the noise transmission facility.

Received Jan. 29, 1982. This paper is the work of the U.S. Government and therefore is in the public domain.

*Aero-Space Technologist. Member AIAA.
†Aero-Space Technologist.
‡Aero-Space Technologist; at present: Senior Acoustics Engineer, Garrett Turbine Engine Co., Phoenix,, Ariz. Member AIAA.
§Professor. Member AIAA.
¶Postdoctoral Research Associate; at present: Member of Technical Staff at Bell Telephone Laboratory, Whippany, N.J.

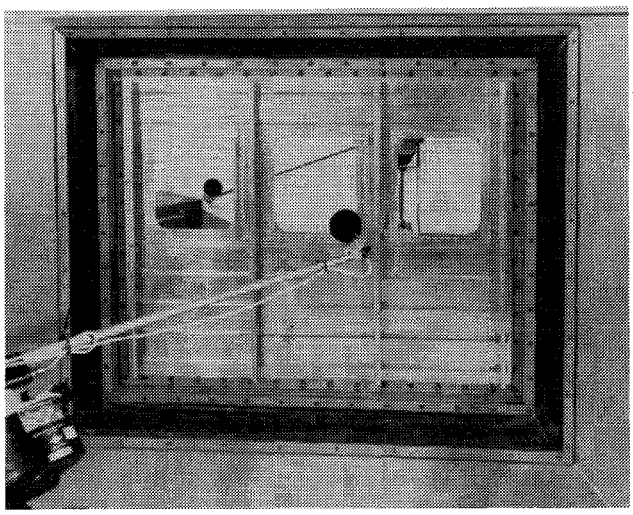

Fig. 2 Panel installation in the TL facility, viewed from the receiving room.

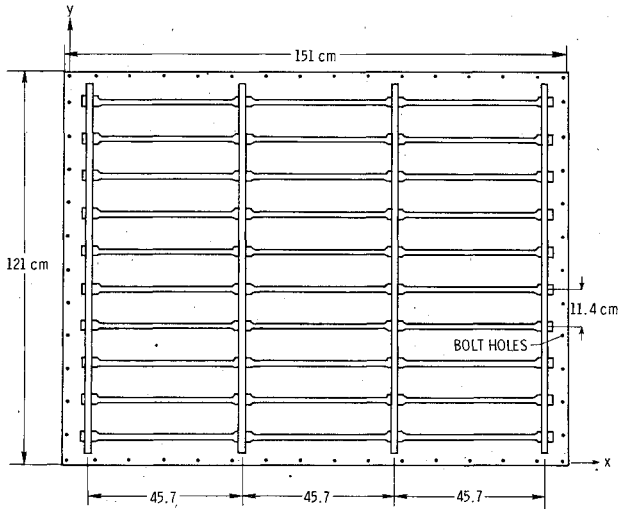

Fig. 3 Dimensions of stiffened aluminum panel. Skin thickness = 0.081 cm.

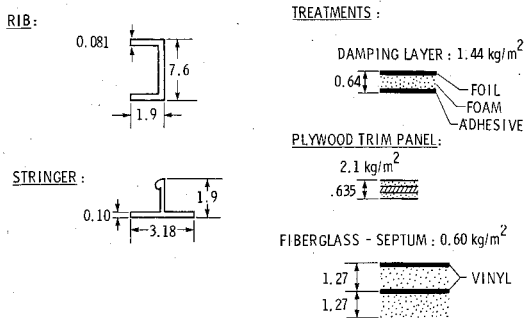

Fig. 4 Details of panel stiffeners and acoustic treatment materials.

to the inside edge of the clamping frame. The panel rib and stringer stiffeners were not clamped along the panel edges.

The fiberglass treatment was installed in between the ribs and over the stringers, leaving about 1.91 cm airspace between panel skin and fiberglass. The fiberglass was held in place with tape, with the fiberglass side toward the skin. The damping layer was installed on the unstiffened side of the skin and was applied uniformly over the whole exposed area using its own adhesive material. The plywood trim panel was supported along its edges by the test window structure. It was not in contact with the panel stiffening ribs and was about 9.14 cm from the skin.

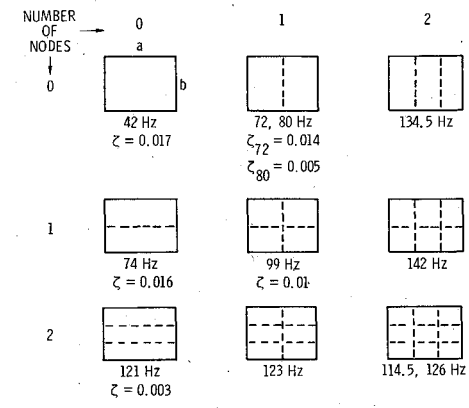

Fig. 5 Resonant frequency, damping, and node line sketches for the stiffened panel.

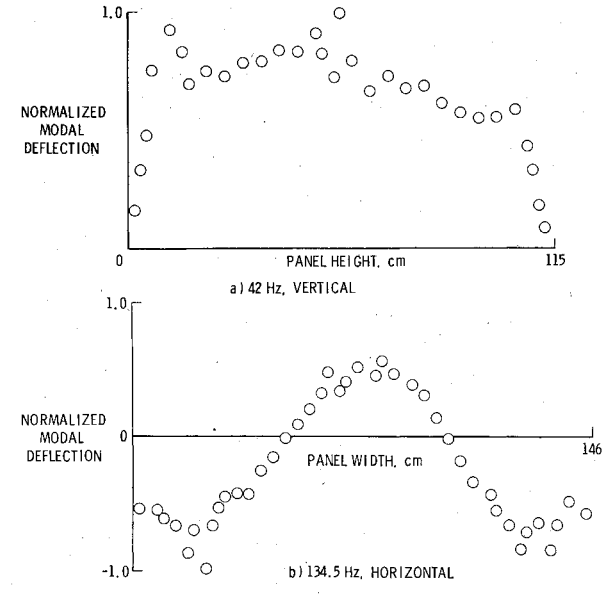

Fig. 6 Mode shapes of the stiffened panel.

Table 1 Panel and treatment configurations

Configuration	Total mass kg/m^2	Treatment[a]
1	4.06	No treatment
2	5.51	Damping on panel
3	5.26	Fiberglass
4	6.16	Trim panel
5	6.71	Damping on panel + fiberglass
6	7.36	Fiberglass + trim panel
7	8.81	Fiberglass + trim panel + damping on trim
8	9.06	Damping on panel + trim panel + damping on trim
9	10.26	Damping on panel + fiberglass + trim panel + damping on trim

[a] All fiberglass treatments consist of two layers, total thickness = 5.08 cm.

Modal Tests

To determine the dynamic characteristics of the test panel as mounted in the window of the TL facility, modal tests were performed. Resonant frequencies, mode shapes, and damping of the first few panel modes were determined using the impulse method.[6,8]

Modal test results are presented in Figs. 5 and 6. Figure 5 shows rough sketches of the node patterns for the lowest 11 resonant frequencies of the panel. Also shown are damping

values for six of the modes measured using the half-power method.[8] The node patterns and damping values are about as expected considering the near-symmetry and the materials of the panel construction. However, Fig. 5 shows that the 0, 1 node pattern occurs at both 72 and 80 Hz. In addition, the modal frequencies are lower than expected based on theoretical predictions.

Detailed mode shapes suggest that panel flexibility near the boundary is greater than expected. Figure 6 shows that large deflections occur very near the panel boundaries. Other mode shapes[6] show that stiffeners and skin are undergoing motions of the same magnitude. That is, at the frequencies indicated, the stiffeners have substantial motion and are not acting as small-motion edge supports for the skin panels (the 11.4×45.7-cm panels shown in Fig. 3), as observed for other panel configurations.[4] This panel-stiffener behavior is expected to effect the noise transmission characteristics of the panel.

Theoretical Predictions

Modal Theory

This analysis is based on a normal mode approach, where the governing acoustic and structural equations of motion are solved using a Galerkin-like procedure.[9,10]

The random pressure acting on the panel is taken as a reverberant acoustic field for which the modal joint acceptances are calculated from

$$j^2_{mn}(\omega)=\frac{1}{A_p^2 S_p(\omega)}\int_{A_p}\int_{A_p} S_p(\omega)R_x(\xi,\omega)R_y(\eta,\omega)$$
$$X_{mn}(x_1,y_1)X_{mn}(x_2,y_2)\,dx_1dx_2dy_1dy_2 \qquad (2)$$

where A_p is the panel area; $S_p(\omega)$ is the acoustic pressure spectral density; $R_x(\xi,\omega)$ and $R_y(\eta,\omega)$ are the spatial correlation coefficients corresponding to longitudinal and transverse directions, respectively; X_{mn} are the normal modes; $\xi=x_2-x_1$; and $\eta=y_2-y_1$. For a diffuse reverberant field, the correlation coefficients are given by

$$R_x(\xi,\omega)=(c/\omega\xi)\sin(\omega\xi/c) \qquad (3a)$$

$$R_y(\eta,\omega)=(c/\omega\eta)\sin(\omega\eta/c) \qquad (3b)$$

where c is the speed of sound in the source room. For an elastic panel simply supported on all four edges the modes are $X_{mn}=\sin(m\pi x/L_x)\sin(n\pi y/L_y)$, where L_x and L_y are the panel dimensions. Using a constant spectral density then allows the joint acceptances to be calculated from Eq. (2) in a closed form.[3,11]

The natural frequencies of the orthogonally stiffened panel are determined using the formulas for free vibration of eccentrically stiffened flat plates.[12] In this procedure, the edges are simply supported, the stiffeners are averaged or "smeared out" into an equivalent skin, and the mode shapes are sinusoidal with zero deflection at the boundaries. The in-plane and rotary inertia effects are neglected; however, the location of the resulting equivalent orthotropic layers relative to the skin middle surface is maintained. The smeared model is only valid for those modal frequencies for which the wavelengths of the longitudinal (x) and transverse (y) panel motions are larger than the distances between ribs and stringers. For the panel shown in Fig. 3 and the selected frequency range 100-1122 Hz, such a model is valid to include all the transverse modes and about the first four longitudinal modes. The calculated fundamental frequency is 81 Hz. Measurements indicate a fundamental frequency of 42 Hz. This difference is probably due to the flexibility near the boundaries of the test panel. Since the effects of the boundary flexibility can be expected to decrease at high frequencies, use of sinusoidal modes in the theory is of interest, especially in view of the considerably greater ease of analysis.

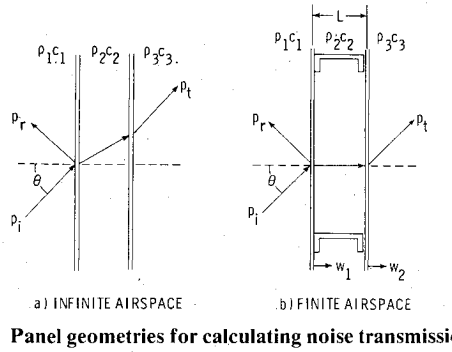

Fig. 7 Panel geometries for calculating noise transmission.

The transmission loss (TL) through the panel is calculated from Eq. (1) where the noise reduction (NR) is calculated using the analytical methods given in Refs. 10 and 11. The transmitted noise is calculated at a point about 127 cm from the center of the panel. Modal damping coefficients are obtained from

$$\zeta_{mn}=\zeta_0\omega_{11}/\omega_{mn}+\zeta^r_{mn} \qquad (4)$$

where $\zeta_0=0.015$ (baseline), $\zeta_0=0.035$ (baseline plus damping tape), ω_{mn} are the natural frequencies, and ζ^r_{mn} are the acoustic radiation damping coefficients.[13] For frequencies below the panel critical frequency, the acoustic radiation damping is very small in comparison to the structural damping. Measured damping values, shown in Fig. 5, tend to agree with the value of ζ_0 and show some decrease of damping in the higher-frequency modes, in agreement with Eq. (4). The noise transmission losses due to added treatments are calculated using the model shown in Fig. 7a and procedures similar to those presented in Refs. 3 and 11. The added transmission loss is obtained from

$$\mathrm{TL}=-10\log[\bar{\tau}(\omega)] \qquad (5)$$

where $\bar{\tau}(\omega)$ is the field incidence transmission coefficient which is calculated by integrating the transmission coefficient $\tau(\theta,\omega)$ over the range of incidence angles using the formula[7]

$$\bar{\tau}(\omega)=2\int_0^{\theta'}\tau(\theta,\omega)\sin(2\theta)\,d\theta/[1-\cos(2\theta')] \qquad (6)$$

where θ' is the limiting value of the incidence angle θ. A value of $\theta'=75$ deg was selected, and integration was performed using a trapezoidal rule with 5-deg angle increments. The transmission coefficient $\tau(\theta,\omega)$ in the integrand of Eq. (6) is calculated from

$$\tau(\theta,\omega)=\left|\frac{(p_1/p_2)_{\mathrm{untr}}}{(p_1/p_2)\ldots(p_{n-1}/p_n)_{\mathrm{tr}}}\right|^2 \qquad (7)$$

where $p_{n-1}p_n$ are the pressure ratios across the different layers of treatment. When calculating the TL of add-on treatments the stiffened aluminum panel is treated as a limp panel having mass of skin and stiffeners averaged over total panel area. The TL of the add-on treatment, Eq. (7), is obtained by subtracting the TL of the limp panel from the TL of the complete layered configuration. This ΔTL was then added to modal theory or mass law theory TL for the stiffened panel to obtain TL of the complete configuration.

Single Panel Mass Law

Sound transmission through a single, limp-mass panel by a plane sound wave at angle θ is given by[7]

$$\tau(\theta,\omega)=[1+(m\omega\cos\theta/2\rho c)^2]^{-1} \qquad (8)$$

where m is the panel mass per unit area and ρc is the characteristic acoustic impedance. For comparison with the

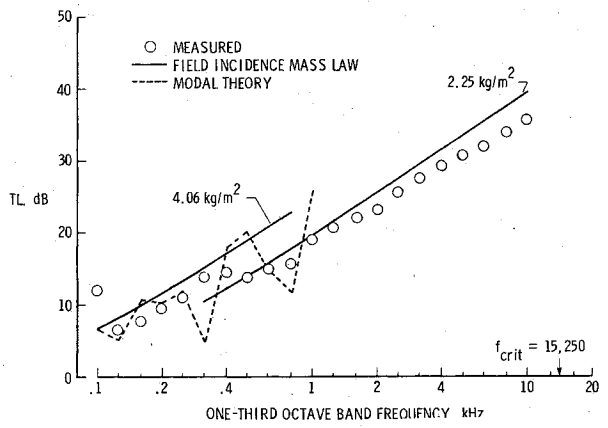

Fig. 8 Transmission loss of the stiffened panel with no treatment.

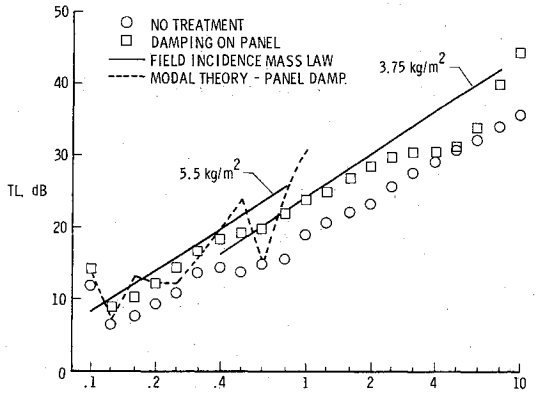

Fig. 9 Transmission loss of the panel without treatment and the panel with damping layer.

experimental diffuse sound field, average transmission coefficient is obtained by substituting $\tau(\theta,\omega)$ given by Eq. (8) into the integrand of Eq. (6) and integrating. Integrating from $\theta = 0$ to 78 deg to obtain a field incidence mass law,[7] results in

$$\bar{\tau}_{fi} = 1.046 b^{-1} \ell_n [(1+b)/(1+0.0432b)] \tag{9}$$

where $b = (m\omega/2\rho c)^2$.

Finite Airspace Double-Wall Mass Law

Previous theories allow wave propagation in the airspace with a component parallel to the panels (Fig. 7a); however, panel stiffeners and the panel boundary framework (Fig. 2) tend to restrict such parallel propagation. In order to evaluate the importance of this effect, the following analysis uses a static approximation for the airspace (Fig. 7b).

Mass is the only physical property assumed for the panels. The length L of the airspace between the panels is assumed to be shorter than the shortest expected wavelength of sound; therefore the airspace is treated as an elemental volume of fluid whose pressure changes are governed by the basic acoustic perturbation equations. Thus the equation for the acoustic pressure in the airspace is given by

$$p_a = \Delta\rho c^2 \tag{10}$$

where $\Delta\rho$ is the change in density of the airspace due to panel motion. The acoustic motion in the airspace is one-dimensional; therefore the mass of an elemental volume is constant. It can be shown that $\Delta\rho$ is given by

$$\Delta\rho = \rho[L/(L+w_2-w_1)-1] \tag{11}$$

where ρ is the ambient density of the undisturbed airspace. Because the panel displacements are much smaller than L, the acoustic pressure in the airspace between the panels reduces to

$$p_a = \rho(w_1 - w_2)c^2/L \tag{12}$$

The remaining governing equations for this system are the differential equation of motion for the left panel,

$$m_1 \ddot{w}_1 = (p_i + p_r)\Big|_{x=0} - p_a \tag{13}$$

the boundary condition on the left side of the left panel,

$$\rho \ddot{w}_1 = -\partial/\partial x (p_i + p_r)\Big|_{x=0} \tag{14}$$

the differential equation of motion for the right panel,

$$m_2 \ddot{w}_2 = -p_t\Big|_{x=L} + p_a \tag{15}$$

and the boundary condition on the right side of the right panel,

$$\rho \ddot{w}_2 = \frac{-\partial p_t}{\partial x}\Big|_{x=L} \tag{16}$$

The assumption that the airspace is small and acts like an element of fluid results in the two boundary conditions at the panel-airspace interfaces being reduced to the single coupling term p_a.

Assuming harmonic plane waves for the incident, reflected and transmitted pressures, and harmonic motion for the panel deflections, substitution into Eqs. (12-16) results in the following four equations governing the motion of the system:

$$(-m_1\omega^2 + \rho c^2/L) W_1 - (\rho c^2/L) W_2 = p_i + p_r \tag{17}$$

$$i\rho c\omega W_1 = (p_i - p_r)\cos(\theta) \tag{18}$$

$$(-m_2\omega^2 + \rho c^2/L) W_2 - (\rho c^2/L) W_1 = -p_t \tag{19}$$

$$i\rho c\omega W_2 = p_t \cos(\theta) \tag{20}$$

Setting the right-hand sides of Eqs. (17) and (19) equal to zero, the solution for ω yields the system's natural frequency f_n:

$$f_n = \frac{1}{2\pi}\sqrt{\frac{\rho c^2}{L}\,\frac{(m_1+m_2)}{m_1 m_2}}$$

Equations (17-20) can be solved for transmission coefficient $\tau(\theta,f)$, which is given by

$$\tau(\theta,f) = \frac{|p_t|^2}{p_i^2} = \left\{\left[\frac{\cos(\theta)\,(m_1+m_2)\,\pi f}{\rho c} \times \left(\frac{f^2}{f_n^2} - 1 - \frac{L\rho}{m_1+m_2}\right)\right]^2 + \left[1 - \frac{f^2}{f_n^2}\,\frac{(m_1+m_2)^2}{2m_1 m_2}\right]^2\right\}^{-1} \tag{21}$$

To find the field incidence transmission coefficient, the quantity $\tau(\theta,f)$, Eq. (21), is integrated (in closed form) over a range of incidence angles.

Conversion to One-Third Octave Bands

For comparison with the experimental data, the transmission coefficient equations must be manipulated to obtain transmission loss averaged over one-third octave bands. Representing mean-square quantities in terms of power spectral density allows for such calculations.[14] The mean-square response $\langle p_i^2(t)\rangle$ associated with a narrow band of frequency Δf is $S(f)\Delta f$, where $S(f)$ is the power spectral density of $\langle p_i^2(t)\rangle$ evaluated at the center frequency of the narrow band. Because $\tau = |p_t|^2/|p_i|^2$, the mean-square response $\langle p_t^2(t)\rangle$ associated with a narrow band Δf is $\tau(f)\,S(f)\Delta f$. So, the transmission loss for a one-third octave band is obtained by adding the narrow bands of incident power and dividing by the sum of the narrow bands of transmitted

power, according to the formula

$$\mathrm{TL} = 10 \log \sum_{f=f_L}^{f_u} S(f)\Delta f \Big/ \sum_{f=f_L}^{f_u} \tau(f) S(f) \Delta f \qquad (22)$$

where f_L is the lower frequency of the one-third octave band, and f_u is the upper frequency of the one-third octave band. For comparison with the data presented herein, the incident pressure spectral density $S(f)$ was experimentally determined, and analytical equations for $\tau(f)$, Eq. (9), for example, were used in Eq. (22) along with the measured $S(f)$ to calculate analytical values of TL in one-third octave bands.

Results and Discussion

Panel Without Treatment

The transmission loss (TL) of the stiffened aluminum panel with no acoustic treatment is shown in Fig. 8. The measured results show that the TL follows two almost straight-line trends with a transition region between about 315 and 630 Hz. The field incidence mass law prediction for 4.06 kg/m^2 was calculated using the mass of stringers and ribs as well as skin, and is shown in the figure to lie parallel to and about 2 dB above the data in the frequency range 125-400 Hz. Modal data showed that the ribs and stringers have vibration motions as large as the skin motions for modes measured up to about 135 Hz. The calculated curve for 2.25 kg/m^2 is based on the mass of skin only, and lies a few dB above the measurements at frequencies above 500 Hz. These results suggest that the panel behavior in these frequency ranges is governed primarily by mass law, and that the components of the panel that govern the transmission are different at different frequencies. This behavior has been observed previously for stiffened panels[7] and is termed "double mass law." The modal theory is in good agreement with the data up to 315 Hz, and has a general upward trend at higher frequency, as do the data.

Single Treatments

Transmission loss is presented in Figs. 9 and 10 for configurations having panel damping, fiberglass, or trim panel treatment. Figure 9 data show that the addition of panel damping treatment raises the transmission loss at all frequencies. The mass law curves are again calculated using the mass of skin, stiffeners, and treatment (5.5 kg/m^2), or only skin and treatment (3.75 kg/m^2). The increase of TL associated with the increase of mass is about 2.6 dB at low frequency and about 4.4 dB at high frequency according to mass law calculations. The measured increases in TL correspond approximately with these mass law predictions, which suggests that the primary contribution of the treatment is its mass, when viewed in one-third octave bands. Narrowband analysis of the data is expected to show a damping effect, also. Modal theory is seen to be in reasonable agreement with the data at low frequencies.

The TL of configurations having either a trim panel or fiberglass treatment is shown in Fig. 10. Figure 10 data show that both trim panel and fiberglass treatments result in a decrease of TL compared to the untreated panel at frequencies between 160 and 315 Hz. At higher frequencies both treatments result in substantial increases of TL over the untreated panel. Over most of the frequency range up to about 1600 Hz, the fiberglass and trim panel have about the same TL even though the trim panel weighs about 2.1 kg/m^2 and the fiberglass weighs 1.2 kg/m^2. Resonances in the airspace between the stiffened panel and the trim panel are calculated to occur at and above about 1900 Hz, which is thought to account for the leveling off of the TL for the "trim panel" curve. Calculated TL is shown in Fig. 10 for modal theory and for normal incidence double-wall mass law. The normal incidence prediction shows a minimum value at 160 Hz associated with the mass-air-mass resonance of the double wall. This falls in the region where the measured results showed a decrease of TL for the fiberglass and trim panel treatments. The difference between modal theory and the data at frequencies from 200 to 315 Hz is thought to be due to differences between the theoretical model (infinite panels and airspace) and the test configuration (finite panels and airspace). The finite airspace analysis addresses part of the differences and is discussed further below.

Combined Treatments

The change of transmission loss associated with combinations of treatments is shown in Figs. 11-13. These results are presented in the form of insertion loss, defined here as the increase of TL that occurs when a particular treatment is added to a configuration that already has an initial treatment. For example, Fig. 11 shows the increase of TL that occurred when a layer of damping material was added to the stiffened panel in configurations having no initial treatment, fiberglass

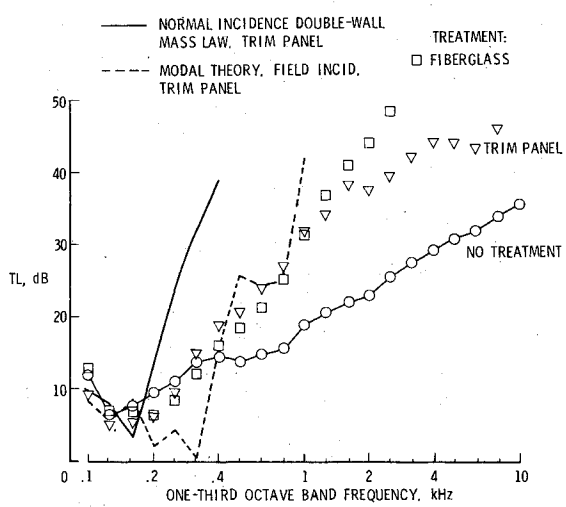

Fig. 10 Effect on transmission loss of trim panel or fiberglass treatment.

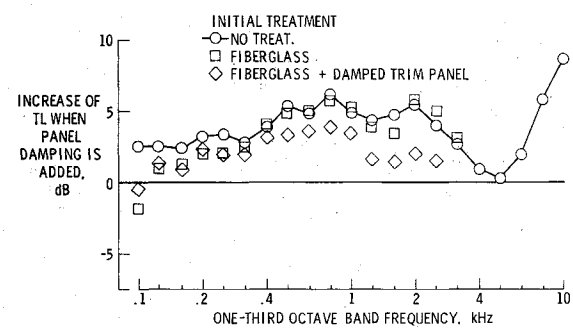

Fig. 11 Insertion loss of panel damping treatment.

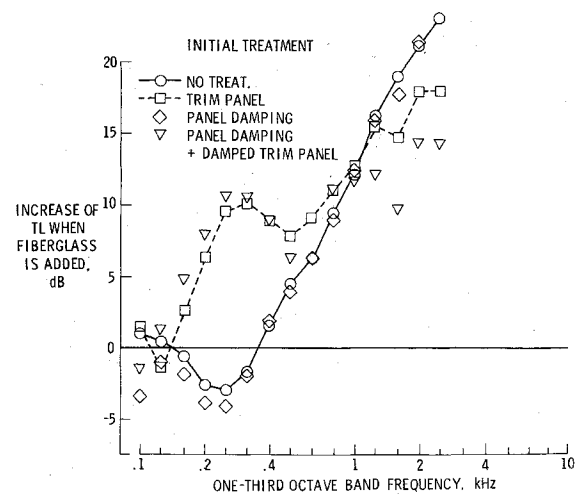

Fig. 12 Insertion loss of fiberglass treatment.

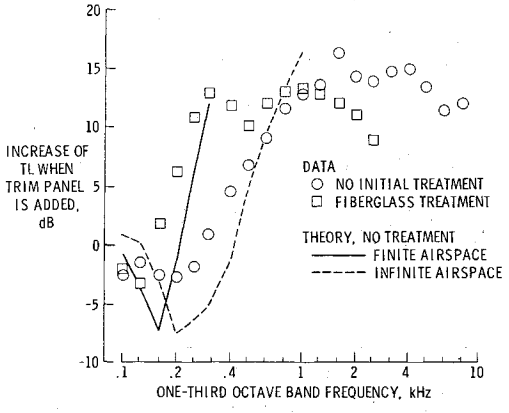

Fig. 13 Insertion loss of trim panel treatment.

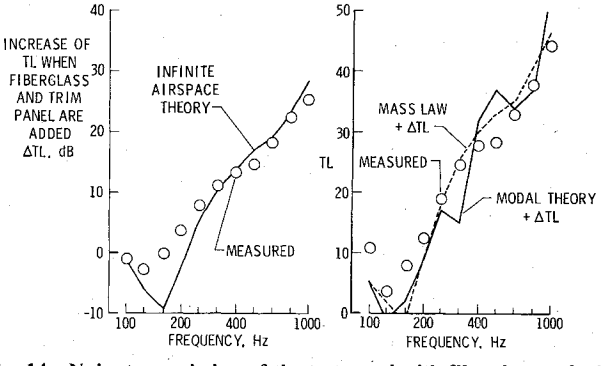

Fig. 14 Noise transmission of the test panel with fiberglass and trim panel treatments.

treatment, or fiberglass plus a damped trim panel treatment. Figure 11 shows that the increase of TL when panel damping is added varies somewhat with frequency and with initial treatment, but generally is less than about 5 dB.

Figure 12 shows that the increase of TL with addition of fiberglass varies by large amounts with both frequency and initial treatment. Addition of fiberglass with either no treatment (solid curve) or panel damping results in a *decrease* of TL at frequencies of from 160 to 315 Hz. In the same frequency range, addition of fiberglass to configurations having a trim panel, the dotted curve, results in *increased* TL by up to about 10 dB. Important propeller harmonics fall in this frequency range for many aircraft. The effect of fiberglass is very nearly the same when the initial treatment is trim panel only (the squares) or panel damping plus damped trim panel (the triangles) even though each of these initial treatments has a different total TL. Similarly, the effect of fiberglass addition is about the same when the initial configuration is either no treatment (circles) or panel damping (diamonds). Figure 9 shows differences of from 2 to 5 dB in the total TL of these two configurations. These results indicate that the effect of adding fiberglass can depend strongly on the initial configuration.

Figure 13 shows the increase of TL resulting from the addition of a trim panel. Results are similar to those for fiberglass. Addition of a trim panel to an untreated panel results in a decrease of TL at low frequencies. However, adding a trim panel to a configuration having fiberglass results in large increases of TL at some low frequencies. Clearly, care must be used when choosing a treatment for a particular application. Modal theory predictions (infinite airspace) in Fig. 13 are in qualitative agreement with data, showing a reduction of TL at low frequencies and large increases of TL at higher frequencies. However, this theory is much lower than the data at frequencies from 200 to 400 Hz. The finite airspace theory predicts higher values of insertion

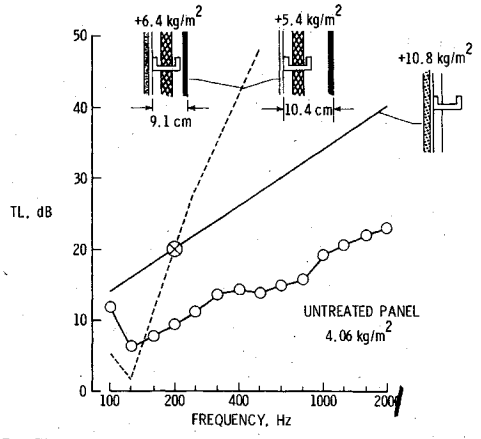

Fig. 15 Side-wall preliminary design for interior noise control.

loss than the infinite airspace theory at frequencies above 160 Hz. Figure 13 indicates that the characteristics of the space between panel and trim are important in determining the transmission loss of the side wall.

Comparisons are shown in Fig. 14 of measured and predicted noise transmission for a configuration having fiberglass and trim panel treatments. The predictions are in reasonable agreement with the data at higher frequencies, but are systematically low at lower frequencies. Incorporation of a finite airspace model is felt likely to improve the prediction.

Figure 15 illustrates the use of the data and theories already presented for a noise control example. The objective was to obtain an additional 10 dB of TL over the untreated panel in the 200-Hz one-third octave band. The addition of mass to the skin was considered to increase the TL according to Eqs. (5) and (8). As shown by the solid line, the addition of 10.8 kg/m^2 (2.2 psf) of mass increased the TL at all frequencies. The finite airspace theory was used to calculate the TL for double-wall designs. The mass required to obtain the 10 dB increase at 200 Hz is less for double walls (dotted line) than for single walls, and is somewhat less for the larger spacing of 10.4 cm. However, the double-wall configurations have very low TL at lower frequencies, which might be a disadvantage depending on the acoustic source spectrum.

Concluding Remarks

This paper describes theoretical and experimental studies of transmission loss of 1.15 × 1.46 m (approximately 4 × 5 ft) flat stiffened panels intended to represent light aircraft construction. Nine configurations were tested having various combinations of a damping layer, a fiberglass-septum layer, and a trim panel.

The untreated panel and the panel with a damping layer on the skin basically followed mass law at frequencies above 100 Hz. The treatments provided substantially increased TL at the higher frequencies; however, the heavier of two treatments did not always provide the greater increase of TL, and the increase of TL provided by the addition of a given treatment depended on the treatment already present in the panel.

Predicted noise transmission (TL and insertion loss) using recently developed modal methods is in reasonable agreement with data at low frequencies for the untreated configurations and at high frequencies for the treated configurations. A simplified analytical model that treats the airspace in the double panel configuration as finite is described in an attempt to improve agreement with data at low frequencies.

References

[1] Revell, J. D., Balena, F.J., and Koval, L.R., "Analytical Study of Interior Noise Control by Fuselage Design Techniques on High Speed, Propeller-Driven Aircraft," NASA CR 159222, July 1978.

[2] Vaicaitis, R., Chang, M.T., and Slazak, M., "Noise Transmission and Attenuation for Business Aircraft," SAE Paper 810561, April 1981.

[3] Rennison, D.C., Wilby, J.F., Marsh, A.H., and Wilby, E.G., "Interior Noise Control Prediction Study for High-Speed Propeller-Drive Aircraft," NASA CR 159200, 1979.

[4] Barton, C.K. and Mixson, J.S., "Noise Transmission and Control for a Light Twin-Engine Aircraft," *Journal of Aircraft,* Vol. 18, July 1981, pp. 570-575.

[5] Barton, C.K., "Development of a Transmission Loss Test Facility for Light Aircraft Structures," *Proceedings of Noise Con 81,* Noise Control Foundation, New York, 1981, pp. 265-268.

[6] Mixson, J.S., Roussos, L.A., Barton, C.K., Vaicaitis, R., and Slazak, M., "Laboratory Study of Efficient Add-On Treatments for Interior Noise Control in Light Aircraft," AIAA Paper 81-1969, Oct. 1981.

[7] Beranek, L.L., ed., *Noise and Vibration Control,* McGraw-Hill, New York, 1971.

[8] Lang, G.F., "Understanding Vibration Measurements," Application Note 9, Nicolet Scientific Corporation, Northvale, N.J., Dec. 1978.

[9] Vaicaitis, R., "Noise Transmission Into a Light Aircraft," *Journal of Aircraft,* Vol. 17, Feb. 1980, pp. 81-86.

[10] Vaicaitis, R. and Slazak, M., "Noise Transmission Through Stiffened Panels," *Journal of Sound and Vibration,* Vol. 70, No. 3, 1980, pp. 413-426.

[11] Cockburn, J.A. and Jolly, A.C., "Structural-Acoustic Response, Noise Transmission Losses and Interior Noise Levels of an Aircraft Fuselage Excited by Random Pressure Fields," AFFDL-TR-68-2, 1968.

[12] Mikulas, M.M. and McElman, J.A., "On Free Vibration of Eccentrically Stiffened Cylindrical Shells and Flat Plates," NASA TN D-3010, 1965.

[13] Smith, P.W. Jr. and Lyon, R.M., "Sound and Structural Vibration," NASA CR-160, 1965.

[14] Robson, J.D., *An Introduction to Random Vibration,* Edinburgh University Press, Edinburgh, Scotland, 1963.